

Muonium-Antimuonium Oscillations in an extended Minimal Supersymmetric Standard Model with right-handed neutrinos

Boyang Liu*

Department of Physics, Purdue University, West Lafayette, IN 47906, USA

Abstract

The electron and muon number violating muonium-antimuonium oscillation process in an extended Minimal Supersymmetric Standard Model is investigated. Modifying the Minimal Supersymmetric Standard Model by the inclusion of three right-handed neutrino superfields and allowing only intra-generation lepton number violation but not inter-generation lepton number mixing, the muonium-antimuonium conversion can occur while the process $\mu \rightarrow e\gamma$ is forbidden. For a wide range of the parameters, the contributions to the muonium-antimuonium oscillation time scale are at least two orders of magnitude below the sensitivity of current experiments. However, if the ratio of the two Higgs field VEVs, $\tan\beta$, is very small, there is a limited possibility that the contributions are large enough for the present experimental limit to provide an inequality relating $\tan\beta$ with the light neutrino mass scale m_ν which is generated by see-saw mechanism. The resultant lower bound on $\tan\beta$ as a function of m_ν is more stringent than the analogous bounds arising from the muon and electron anomalous magnetic moments as computed using this model.

1 Introduction

The time-dependent oscillation between two distinct levels or particle species is an interesting quantum mechanical phenomenon which has been widely studied in many physical systems varying from a particle moving in a double-well potential of the ammonia molecule to oscillations in the neutral $K^0 - \bar{K}^0$ and $B^0 - \bar{B}^0$ meson systems[1]-[3]. It was suggested roughly 50 years ago[4] that there may be a spontaneous conversion between muonium and antimuonium resulting in an associated oscillation effect. Muonium (M) is the Coulombic bound state of an electron

*liu115@physics.purdue.edu

and an antimuon ($e^-\mu^+$), while antimuonium (\bar{M}) is the Coulombic bound state of a positron and a muon ($e^+\mu^-$). Since it has no hadronic constituents, muonium is an ideal place to test electroweak interactions. Of particular interest is that such a muonium-antimuonium oscillation is totally forbidden within the Standard Model because the process violates the individual electron and muon number conservation laws by two units. Hence, its observation will be a clear signal of physics beyond the Standard Model. Since the initial suggestion, experimental searches have been conducted[5]-[6] and a variety of theoretical models have been proposed which can give rise to such a muonium-antimuonium conversion. These include interactions which can be mediated by (a) a doubly charged Higgs boson Δ^{++} [7, 8], which is contained in a left-right symmetric model, (b) massive Majorana neutrinos[9, 10, 11], or (c) the τ -sneutrino in an R-parity violation supersymmetric model[12].

In this paper we consider the muonium-antimuonium oscillation process in the Minimal Supersymmetric Standard Model extended by the inclusion of three right-handed neutrino superfields and where lepton flavor mixing is absent. This assumption automatically forbids the $\mu \rightarrow e\gamma$ decay, so that the muonium- antimuonium oscillation process can be used to constrain the model parameters. In order for there to be a nontrivial mixing between the muonium and antimuonium, the individual electron and muon number conservation must be violated by two units. Such a situation will result provided that the neutrinos are massive Majorana particles or the mass diagonal sneutrinos are lepton number violating scalar particles.

2 The extended Minimal Supersymmetric Standard Model

The Minimal Supersymmetric Standard Model (MSSM) is the supersymmetric extension of the (2 scalar doublet) Standard Model with the minimal particle content[13]. For each particle, there is a superpartner with the same internal quantum numbers, but with spin that differs by half a unit. Tab. 1 lists all the chiral supermultiplets needed for MSSM,

Names		Spin 0	Spin $\frac{1}{2}$	$\text{SU}(3)_C, \text{SU}(2)_L, \text{U}(1)_Y$
squarks and quarks ($\times 3$ families)	Q	$(\tilde{u}_L \ \tilde{d}_L)$	$(u_{L\alpha} \ d_{L\alpha})$	$(3, 2, \frac{1}{6})$
	U^c	\tilde{u}_R^*	$\bar{u}_R^{\dot{\alpha}}$	$(\bar{3}, 1, -\frac{2}{3})$
	D^c	\tilde{d}_R^*	$\bar{d}_R^{\dot{\alpha}}$	$(\bar{3}, 1, \frac{1}{3})$
sleptons, leptons ($\times 3$ families)	L	$(\tilde{\nu}_L \ \tilde{e}_L)$	$(\nu_{L\alpha} \ e_{L\alpha})$	$(1, 2, -\frac{1}{2})$
	E^c	\tilde{e}_R^*	$\bar{e}_R^{\dot{\alpha}}$	$(1, 1, 1)$
Higgs, higgsinos	H_T	$(h_T^+ \ h_T^0)$	$(\tilde{h}_{T\alpha}^+ \ \tilde{h}_{T\alpha}^0)$	$(1, 2, \frac{1}{2})$
	H_B	$(h_B^0 \ h_B^-)$	$(\tilde{h}_{B\alpha}^0 \ \tilde{h}_{B\alpha}^-)$	$(1, 2, -\frac{1}{2})$

Table 1: Chiral supermultiplets of the MSSM

while Tab. 2 summarizes the gauge supermultiplets of MSSM.

Names	Spin $\frac{1}{2}$	Spin 1	$\text{SU}(3)_C, \text{SU}(2)_L, \text{U}(1)_Y$
Gluino, gluon	\tilde{g}_α	g_μ	$(8, 1, 0)$
winos, W bosons	$\tilde{W}_\alpha^\pm \ \tilde{W}_\alpha^0$	$W_\mu^\pm \ W_\mu^0$	$(1, 3, 0)$
bino, B boson	\tilde{B}_α	B_μ	$(1, 1, 0)$

Table 2: Gauge supermultiplets in the MSSM

In the above two tables, the dotted and undotted indices, $\alpha, \dot{\alpha}$, indicate 2-component Weyl spinor fields. In the subsequent analysis, we will recast all the spin $\frac{1}{2}$ fields as 4-component Dirac spinor fields, which will be represented using the same symbols, but without the dotted and undotted “ α ”s. For example, $\nu_{L\alpha}$ is the Weyl representation of the left-handed neutrino field, while $\nu_L = \begin{pmatrix} \nu_{L\alpha} \\ \bar{\nu}_L^{\dot{\alpha}} \end{pmatrix}$ is the Dirac field.

In order to implement the see-saw mechanism[14] for neutrino masses, we consider an extension of the MSSM, where one adds three additional gauge singlet chiral superfields N_i^c ($i=e, \mu, \tau$ denotes the generation), whose θ -component is a right-handed neutrino field,

$$N_i^c = \tilde{\nu}_{iR}^*(y) + \sqrt{2}\theta^\alpha \nu_{R(y)\alpha} + \theta^\alpha \theta_\alpha F_{N_i^c}(y), \quad (1)$$

where

$$y^\mu = x^\mu + i\theta^\alpha \sigma_{\alpha\dot{\alpha}}^\mu \bar{\theta}^{\dot{\alpha}}. \quad (2)$$

These $SU(3) \times SU(2)_L \times U(1)$ singlet superfields are coupled to other MSSM superfields via the superpotential. We employ the most general R-parity conserving renormalizable superpotential so that the superpotential is

$$W = -\mu\epsilon_{ab}H_B^a H_T^b + \lambda_i\epsilon_{ab}E_i^c L_i^a H_B^b + \lambda'_i\epsilon_{ab}H_T^a L_i^b N_i^c + \frac{1}{2}M_R^i N_i^c N_i^c, \quad (3)$$

while the relevant soft supersymmetry breaking terms are

$$\begin{aligned} \mathcal{L}_{soft}^{EMSSM} = & -(m_L^i)^2 (\tilde{v}_{iL}^* \tilde{v}_{iL} + \tilde{\ell}_{iL}^* \tilde{\ell}_{iL}) - (m_R^i)^2 \tilde{\ell}_{iR}^* \tilde{\ell}_{iR} - (m_N^i)^2 \tilde{v}_{iR}^* \tilde{v}_{iR} \\ & - (\lambda'_i A_i h_T^0 \tilde{v}_{iL} \tilde{v}_{iR}^* + M_R^i B_i \tilde{v}_{iR} \tilde{v}_{iR} + \lambda_i C_i h_B^0 \tilde{\ell}_{iL} \tilde{\ell}_{iR}^* + H.C.). \end{aligned} \quad (4)$$

The interaction terms that contribute to the muonium-antimuonium oscillation and the electron and muon anomalous magnetic moments can be extracted from the Lagrangian of this extended Minimal Supersymmetric Standard Model (EMSSM) as

$$\mathcal{L}_{int}^W = -\frac{g_2}{\sqrt{2}} (W^{-\mu} \tilde{\ell}_{iL} \gamma_\mu \nu_{iL} + W^{+\mu} \tilde{\nu}_{iL} \gamma_\mu \ell_{iL}), \quad (5)$$

$$\mathcal{L}_{int}^{\tilde{W}^-} = -ig_2 (\tilde{\ell}_{iL} \tilde{W}^- \tilde{\nu}_{iL} - \tilde{\nu}_{iL}^* \overline{\tilde{W}^-} \ell_{iL}), \quad (6)$$

$$\mathcal{L}_{int}^{\tilde{W}^0} = \frac{g_2 i}{\sqrt{2}} (\tilde{\ell}_{iL} \tilde{W}^0 \tilde{\ell}_{iL} - \tilde{\ell}_{iL}^* \overline{\tilde{W}^0} \ell_{iL}), \quad (7)$$

$$\mathcal{L}_{int}^{\tilde{B}} = \frac{g_1 i}{\sqrt{2}} (\tilde{\ell}_{iL} \tilde{B} \tilde{\ell}_{iL} - \tilde{\ell}_{iL}^* \overline{\tilde{B}} \ell_{iL}) + \sqrt{2} g_1 i (\tilde{\ell}_{iR} \tilde{B} \tilde{\ell}_{iR} - \tilde{\ell}_{iR}^* \overline{\tilde{B}} \ell_{iR}), \quad (8)$$

$$\mathcal{L}_{int}^{\tilde{h}_B^-} = \frac{m_i}{V_B} (\tilde{\ell}_{iR} \tilde{h}_B^- \tilde{\nu}_{iL} + \overline{\tilde{h}_B^-} \ell_{iR} \tilde{\nu}_{iL}^*) + \frac{m_D^i}{V_T} (\tilde{\ell}_{iL} \tilde{h}_B^- \tilde{\nu}_{iR} + \overline{\tilde{h}_B^-} \ell_{iL} \tilde{\nu}_{iR}^*), \quad (9)$$

$$\mathcal{L}_{int}^{\tilde{h}_B^0} = -\frac{m_i}{V_B} (\tilde{\ell}_{iL} \tilde{h}_B^0 \tilde{\ell}_{iR} + \tilde{\ell}_{iR}^* \overline{\tilde{h}_B^0} \ell_{iL}) - \frac{m_i}{V_B} (\tilde{\ell}_{iR} \tilde{h}_B^0 \tilde{\ell}_{iL} + \tilde{\ell}_{iL}^* \overline{\tilde{h}_B^0} \ell_{iR}). \quad (10)$$

In the above equations, all the spin $\frac{1}{2}$ fields are Dirac spinor fields. In particular, note that the field \tilde{h}_B^- has the Weyl field decomposition

$$\tilde{h}_B^- = \begin{pmatrix} \tilde{h}_{B\alpha}^- \\ \overline{\tilde{h}_T^+}^{\dot{\alpha}} \end{pmatrix}. \quad (11)$$

The parameters V_B and V_T are the vacuum expectation values of the two Higgs fields: $\langle h_B^0 \rangle = V_B$ and $\langle h_T^0 \rangle = V_T$. These VEVs are related to the known mass of the W boson and the electroweak gauge couplings as

$$V_B^2 + V_T^2 = V^2 = \frac{2M_W^2}{g_2^2} \approx (174 \text{ GeV})^2, \quad (12)$$

while the ratio of the VEVs is traditionally written as

$$\tan\beta \equiv \frac{V_T}{V_B}. \quad (13)$$

In the above, $m_D^i = \lambda'_i V_T$ are the Dirac mass parameters of neutrinos and m_i are the lepton masses. Since the masses of electron and muon are small, the terms which have couplings proportional to m_i/V_B in interactions (9) and (10) are severely suppressed and will be ignored in the subsequent analysis.

The neutrino mass term can be extracted from the superpotential terms $\lambda'_i \epsilon_{ab} H_T^a L_i^b N_i^c$ and $\frac{1}{2} M_R^i N_i^c N_i^c$ as

$$\mathcal{L}_{mass}^{\nu_i} = -\frac{1}{2} \left(\overline{(v_{iL})^c} \quad \overline{v_{iR}} \right) \begin{pmatrix} 0 & m_D^i \\ m_D^i & M_R^i \end{pmatrix} \begin{pmatrix} v_{iL} \\ (v_{iR})^c \end{pmatrix} + H.C. \quad (14)$$

Note that the upper left element in the neutrino mass matrix is zero. This element involves only left-handed neutrinos and in our EMSSM its generation requires a nonrenormalizable superpotential term. Consequently we ignore this term. For every generation, the two mass eigenvalues, $m_a^{\nu_i}$, are obtained from the diagonalization of the 2×2 matrix

$$M^{\nu_i} = \begin{pmatrix} 0 & m_D^i \\ m_D^i & M_R^i \end{pmatrix}. \quad (15)$$

Since M^{ν_i} is symmetric, it can be diagonalized by a single unitary 2×2 matrix, V^i , as

$$M_{diag}^{\nu_i} = V^{iT} M^{\nu_i} V^i. \quad (16)$$

This diagonalization is implemented via the basis change as following

$$\begin{pmatrix} v_{iL} \\ (v_{iR})^c \end{pmatrix} = V^i \begin{pmatrix} v_{i1} \\ (v_{i2})^c \end{pmatrix}, \quad \begin{pmatrix} (v_{iL})^c \\ v_{iR} \end{pmatrix} = V^{i*} \begin{pmatrix} (v_{i1})^c \\ v_{i2} \end{pmatrix}. \quad (17)$$

The neutrino mass term then takes the form

$$\mathcal{L}_{mass}^{\nu_i} = -\frac{1}{2} \sum_{a=1}^2 m_A^{\nu_i} [v_{ia}^T C v_{ia} + \overline{v_{ia}} C \overline{v_{ia}^T}] = -\sum_{a=1}^2 m_a^{\nu_i} \overline{v_{ia}} v_{ia}, \quad (18)$$

where $m_A^{\nu_i}$ are the Majorana neutrino masses.

Since a nonzero Majorana mass parameter M_R^i does not require $SU(2)_L \times U(1)$ symmetry breaking, it's naturally much bigger than the Dirac mass parameter m_D^i whose nontrivial value

does require $SU(2)_L \times U(1)$ symmetry breaking. So doing, one finds on diagonalization of the 2×2 neutrino mass matrix that the two eigenvalues are crudely given by

$$m_1^{V_i} \sim \frac{(m_D^i)^2}{M_R^i} \ll m_D^i, \quad m_2^{V_i} \sim M_R^i. \quad (19)$$

This constitutes the so called see-saw mechanism[14] and provides a natural explanation of the smallness of the three light neutrino masses. Moreover, the elements of the mixing matrix are characterized by an m_D^i/M_R^i dependence. We expand V^i in power series of the matrix parameter $\xi_i = \frac{m_D^i}{M_R^i}$, with the constraint $\xi_i \ll 1$. The form of V^i to first order in ξ_i can be estimated to be

$$V^i = \begin{pmatrix} 1 & \xi_i \\ -\xi_i & 1 \end{pmatrix}. \quad (20)$$

The sneutrino masses are obtained by diagonalizing a 4×4 squared mass matrix. Here, it's convenient to define $\tilde{\nu}_{iL} = \frac{1}{\sqrt{2}}(\tilde{\nu}_{iL1} + i\tilde{\nu}_{iL2})$ and $\tilde{\nu}_{iR} = \frac{1}{\sqrt{2}}(\tilde{\nu}_{iR1} + i\tilde{\nu}_{iR2})$. Then, the sneutrino-squared mass matrix separates into CP-even and CP-odd blocks[15],

$$\begin{aligned} \mathcal{L}_{mass}^{\tilde{\nu}_i} &= \frac{1}{2} \begin{pmatrix} \phi_1^i & \phi_2^i \end{pmatrix} \mathcal{M}_{\tilde{\nu}_i}^2 \begin{pmatrix} \phi_1^i \\ \phi_2^i \end{pmatrix} \\ &= \frac{1}{2} \begin{pmatrix} \phi_1^i & \phi_2^i \end{pmatrix} \begin{pmatrix} \mathcal{M}_{\tilde{\nu}_i+}^2 & 0 \\ 0 & \mathcal{M}_{\tilde{\nu}_i-}^2 \end{pmatrix} \begin{pmatrix} \phi_1^i \\ \phi_2^i \end{pmatrix}, \end{aligned} \quad (21)$$

where $\phi_a^i \equiv (\tilde{\nu}_{iLa} \ \tilde{\nu}_{iRa})$ and $\mathcal{M}_{\tilde{\nu}_i\pm}^2$ consist of the following 2×2 blocks:

$$\mathcal{M}_{\tilde{\nu}_i\pm}^2 = \begin{pmatrix} (m_L^i)^2 + \frac{1}{2}m_Z^2 \cos 2\beta + (m_D^i)^2 & m_D^i(A_i - \mu \cot \beta \pm M_R^i) \\ m_D^i(A_i - \mu \cot \beta \pm M_R^i) & (M_R^i)^2 + (m_D^i)^2 + (m_N^i)^2 \pm 2B_i M_R^i \end{pmatrix}, \quad (22)$$

with A_i and B_i are SUSY breaking parameters (cf. Eq.(4)). Since the sneutrino mass matrix $\mathcal{M}_{\tilde{\nu}_i}^2$ is real and symmetric, it can be diagonalized by a real orthogonal 4×4 matrix, U^i , as

$$\mathcal{M}_{\tilde{\nu}_i diag}^2 = U^{iT} \mathcal{M}_{\tilde{\nu}_i}^2 U^i, \quad (23)$$

where U^i is in a form as

$$U^i = \begin{pmatrix} U_+^i & 0 \\ 0 & U_-^i \end{pmatrix}. \quad (24)$$

This diagonalization is implemented via the basis change on ϕ_1^i and ϕ_2^i

$$\begin{pmatrix} \phi_1^i \\ \phi_2^i \end{pmatrix} = \begin{pmatrix} \tilde{\nu}_{iL1} \\ \tilde{\nu}_{iR1} \\ \tilde{\nu}_{iL2} \\ \tilde{\nu}_{iR2} \end{pmatrix} = U^i \begin{pmatrix} \tilde{\nu}_{i1} \\ \tilde{\nu}_{i2} \\ \tilde{\nu}_{i3} \\ \tilde{\nu}_{i4} \end{pmatrix}, \quad (25)$$

where $\tilde{\nu}_{ia}$ are all real. Then the sneutrino mass term takes the form

$$\mathcal{L}_{mass}^{\tilde{\nu}_i} = -\frac{1}{2} \sum_{a=1}^4 m_a^{\tilde{\nu}_i} \tilde{\nu}_{ia} \tilde{\nu}_{ia}, \quad (26)$$

where $m_a^{\tilde{\nu}_i}$ are the sneutrino mass eigenvalues.

In the following derivation we assume that M_R^i is the largest mass parameter. Then, to the first order in $1/M_R^i$, the two light mass eigenvalues are roughly

$$\begin{aligned} m_{\tilde{\nu}_{i1}}^2 &\approx (m_L^i)^2 + \frac{1}{2} m_Z^2 \cos 2\beta - \frac{2(m_D^i)^2 (A_i - \mu \cot \beta - B_i)}{M_R^i}, \\ m_{\tilde{\nu}_{i3}}^2 &\approx (m_L^i)^2 + \frac{1}{2} m_Z^2 \cos 2\beta + \frac{2(m_D^i)^2 (A_i - \mu \cot \beta - B_i)}{M_R^i}, \end{aligned} \quad (27)$$

while the two heavy mass eigenvalues are

$$\begin{aligned} m_{\tilde{\nu}_{i2}}^2 &\approx (M_R^i)^2 + 2B_i M_R^i, \\ m_{\tilde{\nu}_{i4}}^2 &\approx (M_R^i)^2 - 2B_i M_R^i. \end{aligned} \quad (28)$$

To avoid excessive complication in our calculations, we expand U^i in powers of the matrix parameter $\xi_i = \frac{m_D^i}{M_R^i}$. The form of U to first order of ξ_i is

$$\begin{aligned} U^i &= \begin{pmatrix} U_+^i & 0 \\ 0 & U_-^i \end{pmatrix} \\ &= \begin{pmatrix} \begin{pmatrix} 1 & \xi_i \\ -\xi_i & 1 \end{pmatrix} & 0 \\ 0 & \begin{pmatrix} 1 & -\xi_i \\ \xi_i & 1 \end{pmatrix} \end{pmatrix}. \end{aligned} \quad (29)$$

For every generation, the slepton mass term is given by

$$\mathcal{L}_{mass}^{\tilde{\ell}_i} = \begin{pmatrix} \tilde{\ell}_{iL} & \tilde{\ell}_{iR}^* \end{pmatrix} \begin{pmatrix} (m_{\tilde{\ell}_i}^{LL})^2 & (m_{\tilde{\ell}_i}^{LR})^2 \\ (m_{\tilde{\ell}_i}^{LR})^2 & (m_{\tilde{\ell}_i}^{RR})^2 \end{pmatrix} \begin{pmatrix} \tilde{\ell}_{iL} \\ \tilde{\ell}_{iR} \end{pmatrix}, \quad (30)$$

where

$$(m_{\tilde{\ell}_i}^{LL})^2 = (m_L^i)^2 + m_Z^2 \cos 2\beta \left(\sin^2 \theta_W - \frac{1}{2} \right), \quad (31)$$

$$(m_{\tilde{\ell}_i}^{LR})^2 = \lambda_i \mu V_T + \lambda_i C_i V_B, \quad (32)$$

$$(m_{\tilde{\ell}_i}^{RR})^2 = (m_R^i)^2 - m_Z^2 \cos 2\beta \sin^2 \theta_W. \quad (33)$$

Since $\lambda_i V_B = m_i$, the off diagonal matrix element, $(m_{\tilde{\ell}_i}^{LR})^2$, can be written as

$$(m_{\tilde{\ell}_i}^{LR})^2 = m_i(\mu \tan \beta + C_i). \quad (34)$$

Because the masses of electron and muon are very small compared with the sparticle mass scale, we ignore these off diagonal terms and consider $\tilde{\ell}_{iL}$ and $\tilde{\ell}_{iR}$ as mass eigenstates.

Inserting the transformation (17) and (25) in the interaction terms (5)-(9) yields the explicit interactions in their mass basis:

$$\mathcal{L}_{int}^W = -\frac{g_2}{\sqrt{2}} \sum_{a=1}^2 \left(W^{-\mu} \tilde{\ell}_{iL} \gamma_\mu V_{1a}^i \nu_{ia} + W^{+\mu} \tilde{\nu}_{ia} V_{1a}^{i*} \gamma_\mu \ell_{iL} \right), \quad (35)$$

$$\mathcal{L}_{int}^{\tilde{W}^-} = -\frac{ig_2}{\sqrt{2}} \sum_{a=1}^2 \tilde{\ell}_{iL} \tilde{W}^- U_{1a}^i \tilde{\nu}_{ia} + \frac{g_2}{\sqrt{2}} \sum_{a=3}^4 \tilde{\ell}_{iL} \tilde{W}^- U_{3a}^i \tilde{\nu}_{ia} + H.C., \quad (36)$$

$$\mathcal{L}_{int}^{\tilde{W}^0} = \frac{g_2 i}{\sqrt{2}} \left(\tilde{\ell}_{iL} \tilde{W}^0 \ell_{iL} - \tilde{\ell}_{iL}^* \tilde{W}^0 \ell_{iL} \right), \quad (37)$$

$$\mathcal{L}_{int}^{\tilde{B}} = \frac{g_1 i}{\sqrt{2}} \left(\tilde{\ell}_{iL} \tilde{B} \ell_{iL} - \tilde{\ell}_{iL}^* \tilde{B} \ell_{iL} \right) + \sqrt{2} g_1 i \left(\tilde{\ell}_{iR} \tilde{B} \ell_{iR} - \tilde{\ell}_{iR}^* \tilde{B} \ell_{iR} \right), \quad (38)$$

$$\mathcal{L}_{int}^{\tilde{h}_B^-} = \frac{m_D^i}{\sqrt{2} V_T} \sum_{a=1}^2 \tilde{\ell}_{iL} \tilde{h}_B^- U_{2a}^i \tilde{\nu}_{ia} + \frac{im_D^i}{\sqrt{2} V_T} \sum_{a=3}^4 \tilde{\ell}_{iL} \tilde{h}_B^- U_{4a}^i \tilde{\nu}_{ia} + H.C.. \quad (39)$$

3 The muonium-antimuonium oscillation in the EMSSM

The lowest order Feynman diagrams accounting for muonium and antimuonium mixing are displayed in Fig.1. Graphs (a) and (b) are the non-SUSY contributions, which are mediated by Majorana neutrinos and W boson. The other graphs all involve SUSY partners. Graphs (c) and (d) are mediated by sneutrinos and wino, while graph (e) and (f) are mediated by sneutrinos and higgsino.

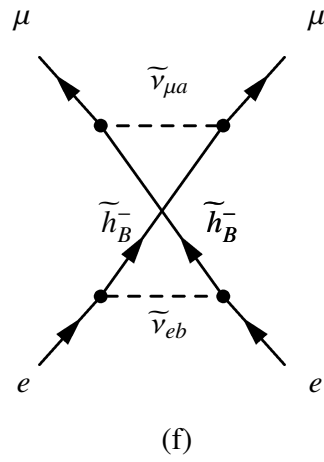
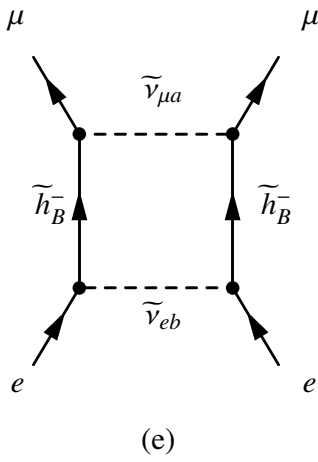
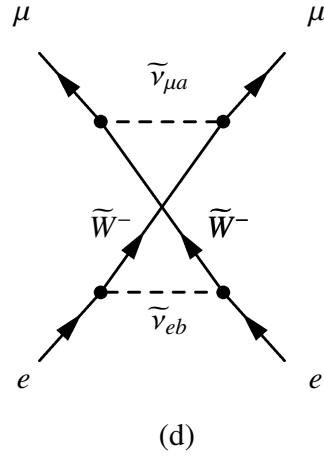
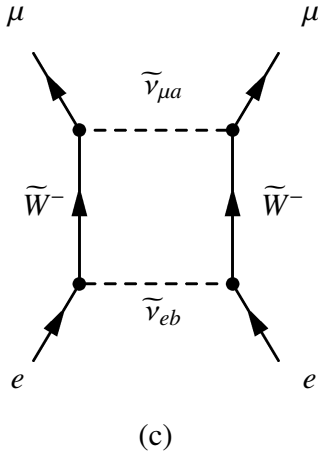
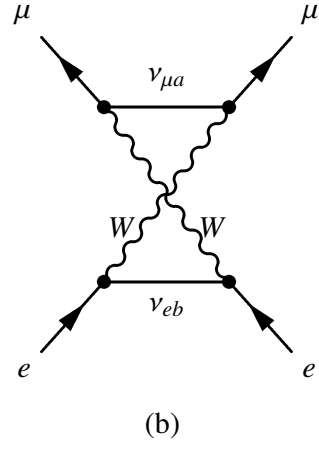
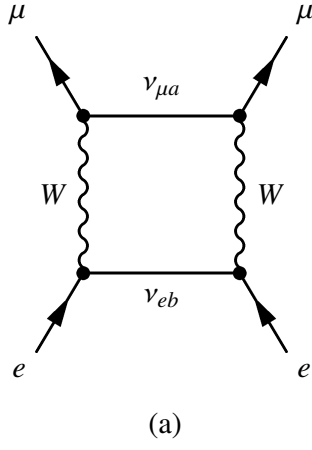


Figure 1: Feynman graphs contributing to the muonium-antimuonium mixing.

The T-matrix elements of graphs (a) and (b) are

$$T_a = T_b = \frac{g_2^4}{512\pi^2 M_W^2} [\bar{\mu}(3)\gamma^\mu(1-\gamma_5)e(2)][\bar{\mu}(4)\gamma_\mu(1-\gamma_5)e(1)] \cdot \sum_{a=1}^2 \sum_{b=1}^2 (V_{1a}^\mu)^2 (V_{1b}^{e*})^2 K(x_{\nu_{\mu a}}, x_{\nu_{eb}}), \quad (40)$$

where $\bar{\mu}(3) = \bar{\mu}(p_3, s_3)$, $\bar{\mu}(4) = \bar{\mu}(p_4, s_4)$, $e(1) = e(p_1, s_1)$ and $e(2) = e(p_2, s_2)$ are the spinors of the muons and electrons and $x_{\nu_{ia}} = \frac{m_{\nu_{ia}}^2}{M_W^2}$, $a = 1, 2$. The function $K(x_{\nu_{\mu a}}, x_{\nu_{eb}})$ takes the form

$$K(x_A, x_B) = \sqrt{x_A x_B} \frac{L(x_A, x_B) - L(x_B, x_A)}{x_A - x_B}, \quad (41)$$

with

$$L(x_A, x_B) = \frac{4 - x_A x_B}{(x_A - 1)} + \frac{x_A(2x_B - x_A x_B - 4)}{(x_A - 1)^2} \ln x_A. \quad (42)$$

The T-matrix elements of graphs (c) and (d) are

$$T_c = T_d = -\frac{g_2^4}{1024\pi^2 M_{\tilde{W}^-}^2} [\bar{\mu}(3)\gamma^\mu(1-\gamma_5)e(2)][\bar{\mu}(4)\gamma_\mu(1-\gamma_5)e(1)] \cdot \left(\sum_{a=1}^2 \sum_{b=1}^2 (U_{1a}^\mu)^2 (U_{1b}^e)^2 I(y_{\tilde{\nu}_{\mu a}}, y_{\tilde{\nu}_{eb}}) - \sum_{a=1}^2 \sum_{b=3}^4 (U_{1a}^\mu)^2 (U_{3b}^e)^2 I(y_{\tilde{\nu}_{\mu a}}, y_{\tilde{\nu}_{eb}}) - \sum_{a=3}^4 \sum_{b=1}^2 (U_{3a}^\mu)^2 (U_{1b}^e)^2 I(y_{\tilde{\nu}_{\mu a}}, y_{\tilde{\nu}_{eb}}) + \sum_{a=3}^4 \sum_{b=3}^4 (U_{3a}^\mu)^2 (U_{3b}^e)^2 I(y_{\tilde{\nu}_{\mu a}}, y_{\tilde{\nu}_{eb}}) \right), \quad (43)$$

where

$$y_{\tilde{\nu}_{ia}} = \frac{m_{\tilde{\nu}_{ia}}^2}{M_{\tilde{W}^-}^2}, \quad (44)$$

$$I(x_1, x_2) = \frac{J(x_1) - J(x_2)}{x_1 - x_2}, \quad (45)$$

with

$$J(x) = \frac{x^2 \ln x - x + 1}{(x - 1)^2}. \quad (46)$$

Finally, the T-matrix elements of graphs (e) and (f) are

$$T_e = T_f = -\frac{(m_D^\mu)^2 (m_D^e)^2}{1024 V_T^4 \pi^2 M_{\tilde{h}_B^-}^2} [\bar{\mu}(3)\gamma^\mu(1-\gamma_5)e(2)][\bar{\mu}(4)\gamma_\mu(1-\gamma_5)e(1)] \cdot \left(\sum_{a=1}^2 \sum_{b=1}^2 (U_{2a}^\mu)^2 (U_{2b}^e)^2 I(z_{\tilde{\nu}_{\mu a}}, z_{\tilde{\nu}_{eb}}) - \sum_{a=1}^2 \sum_{b=3}^4 (U_{2a}^\mu)^2 (U_{4b}^e)^2 I(z_{\tilde{\nu}_{\mu a}}, z_{\tilde{\nu}_{eb}}) \right)$$

$$- \sum_{a=3}^4 \sum_{b=1}^2 (U_{4a}^\mu)^2 (U_{2b}^e)^2 I(z_{\tilde{\nu}_{\mu a}}, z_{\tilde{\nu}_{eb}}) + \sum_{a=3}^4 \sum_{b=3}^4 (U_{4a}^\mu)^2 (U_{4b}^e)^2 I(z_{\tilde{\nu}_{\mu a}}, z_{\tilde{\nu}_{eb}}) \Big), \quad (47)$$

where

$$z_{\tilde{\nu}_{ia}} = \frac{m_{\tilde{\nu}_{ia}}^2}{M_{\tilde{h}_B^-}^2}. \quad (48)$$

4 The effective Lagrangian

Combining all the T-matrix elements, we secure an effective Lagrangian which can be cast as:

$$\mathcal{L}_{eff} = \frac{G_{\bar{M}M}}{\sqrt{2}} [\bar{\mu} \gamma^\mu (1 - \gamma_5) e] [\bar{\mu} \gamma_\mu (1 - \gamma_5) e], \quad (49)$$

where

$$\begin{aligned} \frac{G_{\bar{M}M}}{\sqrt{2}} = & \frac{g_2^4}{1024\pi^2 M_W^2} \cdot \sum_{a=1}^2 \sum_{b=1}^2 (V_{1a}^\mu)^2 (V_{1b}^{e*})^2 K(x_{\nu_{\mu a}}, x_{\nu_{eb}}) \\ & - \frac{g_2^4}{2048\pi^2 M_{\tilde{W}^-}^2} \cdot \left(\sum_{a=1}^2 \sum_{b=1}^2 (U_{1a}^\mu)^2 (U_{1b}^e)^2 I(y_{\tilde{\nu}_{\mu a}}, y_{\tilde{\nu}_{eb}}) - \sum_{a=1}^2 \sum_{b=3}^4 (U_{1a}^\mu)^2 (U_{3b}^e)^2 I(y_{\tilde{\nu}_{\mu a}}, y_{\tilde{\nu}_{eb}}) \right. \\ & - \sum_{a=3}^4 \sum_{b=1}^2 (U_{3a}^\mu)^2 (U_{1b}^e)^2 I(y_{\tilde{\nu}_{\mu a}}, y_{\tilde{\nu}_{eb}}) + \sum_{a=3}^4 \sum_{b=3}^4 (U_{3a}^\mu)^2 (U_{3b}^e)^2 I(y_{\tilde{\nu}_{\mu a}}, y_{\tilde{\nu}_{eb}}) \Big) \\ & - \frac{(m_D^\mu)^2 (m_D^e)^2}{2048 V_T^4 \pi^2 M_{\tilde{h}_B^-}^2} \cdot \left(\sum_{a=1}^2 \sum_{b=1}^2 (U_{2a}^\mu)^2 (U_{2b}^e)^2 I(z_{\tilde{\nu}_{\mu a}}, z_{\tilde{\nu}_{eb}}) - \sum_{a=1}^2 \sum_{b=3}^4 (U_{2a}^\mu)^2 (U_{4b}^e)^2 I(z_{\tilde{\nu}_{\mu a}}, z_{\tilde{\nu}_{eb}}) \right. \\ & - \sum_{a=3}^4 \sum_{b=1}^2 (U_{4a}^\mu)^2 (U_{2b}^e)^2 I(z_{\tilde{\nu}_{\mu a}}, z_{\tilde{\nu}_{eb}}) + \sum_{a=3}^4 \sum_{b=3}^4 (U_{4a}^\mu)^2 (U_{4b}^e)^2 I(z_{\tilde{\nu}_{\mu a}}, z_{\tilde{\nu}_{eb}}) \Big). \end{aligned} \quad (50)$$

Muonium (antimuonium) is a nonrelativistic Coulombic bound state of an electron and an anti-muon (positron and muon). The nontrivial mixing between the muonium ($|M\rangle$) and anti-muonium ($|\bar{M}\rangle$) states is encapsulated in the effective Lagrangian of Eq. (49) and leads to the mass diagonal states given by the linear combinations

$$|M_\pm\rangle = \frac{1}{\sqrt{2(1+|\varepsilon|^2)}} [(1+\varepsilon)|M\rangle \pm (1-\varepsilon)|\bar{M}\rangle], \quad (51)$$

where

$$\varepsilon = \frac{\sqrt{\mathcal{M}_{M\bar{M}}} - \sqrt{\mathcal{M}_{\bar{M}M}}}{\sqrt{\mathcal{M}_{M\bar{M}}} + \sqrt{\mathcal{M}_{\bar{M}M}}}, \quad (52)$$

$$\mathcal{M}_{M\bar{M}} = \frac{\langle M | - \int d^3 r \mathcal{L}_{eff} | \bar{M} \rangle}{\sqrt{\langle M | M \rangle \langle \bar{M} | \bar{M} \rangle}}, \quad \mathcal{M}_{\bar{M}M} = \frac{\langle \bar{M} | - \int d^3 r \mathcal{L}_{eff} | M \rangle}{\sqrt{\langle M | M \rangle \langle \bar{M} | \bar{M} \rangle}}. \quad (53)$$

Since the neutrino sector is expected, in general, to be CP violating, these will be independent, complex matrix elements. If the neutrino sector conserves CP, with $|M\rangle$ and $|\bar{M}\rangle$ CP conjugate states, then $\mathcal{M}_{M\bar{M}} = \mathcal{M}_{\bar{M}M}$ and $\epsilon = 0$. In general, the magnitude of the mass splitting between the two mass eigenstates is

$$|\Delta M| = 2 \left| \text{Re} \sqrt{\mathcal{M}_{M\bar{M}} \mathcal{M}_{\bar{M}M}} \right|. \quad (54)$$

Since muonium and antimuonium are linear combinations of the mass diagonal states, an initially prepared muonium or antimuonium state will undergo oscillations into one another as a function of time. The muonium-antimuonium oscillation time scale, $\tau_{\bar{M}M}$, is given by

$$\frac{1}{\tau_{\bar{M}M}} = |\Delta M|. \quad (55)$$

We would like to evaluate $|\Delta M|$ in the nonrelativistic limit. A nonrelativistic reduction of the effective Lagrangian of Eq. (50) produces the local, complex effective potential

$$V_{eff}(\mathbf{r}) = 8 \frac{G_{\bar{M}M}}{\sqrt{2}} \delta^3(\mathbf{r}). \quad (56)$$

Taking the muonium (antimuonium) to be in their respective Coulombic ground states, $\phi_{100}(\mathbf{r}) = \frac{1}{\sqrt{\pi a_{\bar{M}M}^3}} e^{-r/a_{\bar{M}M}}$, where $a_{\bar{M}M} = \frac{1}{m_{red}\alpha}$ is the muonium Bohr radius with $m_{red} = \frac{m_e m_\mu}{m_e + m_\mu} \simeq m_e$ the reduced mass of muonium, it follows that

$$\begin{aligned} \frac{1}{\tau_{\bar{M}M}} &\simeq 2 \int d^3r \phi_{100}^*(\mathbf{r}) | \text{Re} V_{eff}(\mathbf{r}) | \phi_{100}(\mathbf{r}) \\ &= 16 \frac{| \text{Re} G_{\bar{M}M} |}{\sqrt{2}} |\phi_{100}(0)|^2 = \frac{16}{\pi} \frac{| \text{Re} G_{\bar{M}M} |}{\sqrt{2}} \frac{1}{a_{\bar{M}M}^3}. \end{aligned} \quad (57)$$

Thus we secure an oscillation time scale

$$\frac{1}{\tau_{\bar{M}M}} \simeq \frac{16}{\pi} \frac{| \text{Re} G_{\bar{M}M} |}{\sqrt{2}} m_e^3 \alpha^3. \quad (58)$$

5 Estimate of the effective coupling constant

The present experimental limit[6] on the non-observation of muonium-antimuonium oscillation translates into the bound

$$| \text{Re} G_{\bar{M}M} | \leq 3.0 \times 10^{-3} G_F, \quad (59)$$

where $G_F \simeq 1.16 \times 10^{-5} \text{GeV}^{-2}$ is the Fermi scale. This limit can then be used to construct some constraints on the parameters of this model.

For simplicity, we set the neutrino Dirac masses m_D^e, m_D^μ and the right-handed neutrino masses M_R^e, M_R^μ to some common mass scales m_D and M_R respectively. The light neutrino mass scale m_ν is of order m_D^2/M_R , while the heavy neutrino mass scale is of order M_R .

Using these assumptions and taking into account the mixing matrices approximations Eq.(20) and (29), we can simplify the effective coupling constant (50) to a more manageable approximated form. The contribution from graphs (a) and (b) in $G_{\bar{M}M}$ is $\frac{g_2^4}{1024\pi^2 M_W^2} \cdot \sum_{a=1}^2 \sum_{b=1}^2 (V_{1a}^\mu)^2 (V_{1b}^{e*})^2 \cdot K(x_{\nu_{\mu a}}, x_{\nu_{e b}})$. With the limits of $m_{\nu_{\mu 1}}, m_{\nu_{e 1}} \sim O(\frac{m_D^2}{M_R})$ and $m_{\nu_{\mu 2}}, m_{\nu_{e 2}} \sim O(M_R)$, the contribution $(V_{1a}^\mu)^2 (V_{1b}^{e*})^2 K(x_{\nu_{\mu a}}, x_{\nu_{e b}})$ can be approximated as

$$\begin{aligned} (V_{11}^\mu)^2 (V_{11}^{e*})^2 K(x_{\nu_{\mu 1}}, x_{\nu_{e 1}}) &\sim \frac{m_D^4}{M_R^2 M_W^2} \ln\left(\frac{M_R M_W}{m_D^2}\right), \\ (V_{11}^\mu)^2 (V_{12}^{e*})^2 K(x_{\nu_{\mu 1}}, x_{\nu_{e 2}}), \quad (V_{12}^\mu)^2 (V_{11}^{e*})^2 K(x_{\nu_{\mu 2}}, x_{\nu_{e 1}}) &\sim \frac{m_D^8}{M_R^4 M_W^4} \ln\left(\frac{M_R M_W}{m_D^2}\right), \\ (V_{12}^\mu)^2 (V_{12}^{e*})^2 K(x_{\nu_{\mu 2}}, x_{\nu_{e 2}}) &\sim \frac{m_D^4}{M_R^2 M_W^2} \ln\left(\frac{M_R}{M_W}\right). \end{aligned} \quad (60)$$

Taking M_R as the largest mass parameter, the first term and the third term are comparable, while the second one is suppressed by a factor $m_D^4/(M_R^2 M_W^2)$. Therefore, the contribution from graphs (a) and (b) is roughly

$$\begin{aligned} &\frac{g_2^4}{1024\pi^2 M_W^2} \cdot \sum_{a=1}^2 \sum_{b=1}^2 (V_{1a}^\mu)^2 (V_{1b}^{e*})^2 K(x_{\nu_{\mu a}}, x_{\nu_{e b}}) \\ &\approx \frac{g_2^4 m_D^4}{1024\pi^2 M_R^2 M_W^4} \cdot \ln\left(\frac{M_R}{M_W}\right). \end{aligned} \quad (61)$$

The second term in Eq.(50) is the contribution of graph (c) and (d), in which the function $I(y_{\tilde{\nu}_{\mu a}}, y_{\tilde{\nu}_{e b}})$ is a decreasing function of $y_{\tilde{\nu}_{\mu a}}$ and $y_{\tilde{\nu}_{e b}}$. It will be small for heavy sneutrinos. To see this, we employ the approximations (29)

$$\begin{aligned} U_{11}^\mu, U_{11}^e, U_{33}^\mu, U_{33}^e &\sim O(1), \\ U_{12}^\mu, U_{12}^e, U_{34}^\mu, U_{34}^e &\sim O\left(\frac{m_D}{M_R}\right), \end{aligned} \quad (62)$$

so that the terms involving heavy sneutrinos will get an extra suppression from the mixing matrix. Therefore, the contribution of graph (c) and (d) is dominated by the term that only includes the light sneutrinos so that

$$-\frac{g_2^4}{2048\pi^2 M_W^2} \cdot \left(\sum_{a=1}^2 \sum_{b=1}^2 (U_{1a}^\mu)^2 (U_{1b}^e)^2 I(y_{\tilde{\nu}_{\mu a}}, y_{\tilde{\nu}_{e b}}) - \sum_{a=1}^2 \sum_{b=3}^4 (U_{1a}^\mu)^2 (U_{3b}^e)^2 I(y_{\tilde{\nu}_{\mu a}}, y_{\tilde{\nu}_{e b}}) \right)$$

$$\begin{aligned}
& - \sum_{a=3}^4 \sum_{b=1}^2 (U_{3a}^\mu)^2 (U_{1b}^e)^2 I(y_{\tilde{\nu}_{\mu a}}, y_{\tilde{\nu}_{eb}}) + \sum_{a=3}^4 \sum_{b=3}^4 (U_{3a}^\mu)^2 (U_{3b}^e)^2 I(y_{\tilde{\nu}_{\mu a}}, y_{\tilde{\nu}_{eb}}) \\
& \approx - \frac{g_2^4}{2048\pi^2 M_{\tilde{W}^-}^2} \cdot (I(y_{\tilde{\nu}_{\mu 1}}, y_{\tilde{\nu}_{e1}}) - I(y_{\tilde{\nu}_{\mu 1}}, y_{\tilde{\nu}_{e3}}) - I(y_{\tilde{\nu}_{\mu 3}}, y_{\tilde{\nu}_{e1}}) + I(y_{\tilde{\nu}_{\mu 3}}, y_{\tilde{\nu}_{e3}})).
\end{aligned} \tag{63}$$

Employing the squared-mass difference between the two light sneutrinos in Eq.(27), the above expression can be approximated as

$$\begin{aligned}
& - \frac{g_2^4}{2048\pi^2 M_{\tilde{W}^-}^2} \cdot (I(y_{\tilde{\nu}_{\mu 1}}, y_{\tilde{\nu}_{e1}}) - I(y_{\tilde{\nu}_{\mu 1}}, y_{\tilde{\nu}_{e3}}) - I(y_{\tilde{\nu}_{\mu 3}}, y_{\tilde{\nu}_{e1}}) + I(y_{\tilde{\nu}_{\mu 3}}, y_{\tilde{\nu}_{e3}})) \\
& \approx - \frac{g_2^4}{2048\pi^2 M_{\tilde{W}^-}^2} \cdot (y_{\tilde{\nu}_{\mu 1}} - y_{\tilde{\nu}_{\mu 3}})(y_{\tilde{\nu}_{e1}} - y_{\tilde{\nu}_{e3}}) \frac{\partial}{\partial y_{\tilde{\nu}_{\mu 1}}} \frac{\partial}{\partial y_{\tilde{\nu}_{e1}}} I(y_{\tilde{\nu}_{\mu 1}}, y_{\tilde{\nu}_{e1}}) \\
& \approx - \frac{g_2^4}{2048\pi^2 M_{\tilde{W}^-}^2} \cdot \frac{\Delta m_{\tilde{\nu}_{\mu}}^2}{M_{\tilde{W}^-}^2} \cdot \frac{\Delta m_{\tilde{\nu}_e}^2}{M_{\tilde{W}^-}^2} \cdot \frac{\partial}{\partial y_{\tilde{\nu}_{\mu 1}}} \frac{\partial}{\partial y_{\tilde{\nu}_{e1}}} I(y_{\tilde{\nu}_{\mu 1}}, y_{\tilde{\nu}_{e1}}),
\end{aligned} \tag{64}$$

where the squared-mass differences are

$$\begin{aligned}
\Delta m_{\tilde{\nu}_{\mu}}^2 &= \frac{4(m_D^\mu)^2 (A_\mu - \mu \cot \beta - B_\mu)}{M_R^\mu}, \\
\Delta m_{\tilde{\nu}_e}^2 &= \frac{4(m_D^e)^2 (A_e - \mu \cot \beta - B_e)}{M_R^e}.
\end{aligned} \tag{65}$$

Assuming $A_\mu = A_e \equiv A$ and $B_\mu = B_e \equiv B$, the squared-mass differences of light muon sneutrinos and light electron sneutrinos are

$$\Delta m_{\tilde{\nu}_{\mu}}^2 = \Delta m_{\tilde{\nu}_e}^2 \equiv \Delta m_{\tilde{\nu}}^2 = \frac{4m_D^2 (A - \mu \cot \beta - B)}{M_R} \tag{66}$$

so that Eq.(64) then simplifies to

$$- \frac{g_2^4}{2048\pi^2 M_{\tilde{W}^-}^2} \cdot \frac{\Delta m_{\tilde{\nu}_{\mu}}^2}{M_{\tilde{W}^-}^2} \cdot \frac{\Delta m_{\tilde{\nu}_e}^2}{M_{\tilde{W}^-}^2} \cdot \frac{\partial}{\partial y_{\tilde{\nu}_{\mu 1}}} \frac{\partial}{\partial y_{\tilde{\nu}_{e1}}} I(y_{\tilde{\nu}_{\mu 1}}, y_{\tilde{\nu}_{e1}}) \approx - \frac{g_2^4 (\Delta m_{\tilde{\nu}}^2)^2}{2048\pi^2 M_{\tilde{W}^-}^6} \frac{\partial}{\partial y_{\tilde{\nu}_{\mu 1}}} \frac{\partial}{\partial y_{\tilde{\nu}_{e1}}} I(y_{\tilde{\nu}_{\mu 1}}, y_{\tilde{\nu}_{e1}}). \tag{67}$$

The contribution from graph (e) and (f) is not dominated by the terms involving only light sneutrinos even though $I(z_{\tilde{\nu}_{\mu a}}, z_{\tilde{\nu}_{eb}})$ is a decreasing function of $z_{\tilde{\nu}_{\mu a}}$ and $z_{\tilde{\nu}_{eb}}$, because these terms get suppressed by the mixing matrix. The terms including only light sneutrinos $\tilde{\nu}_{\mu 1}$, $\tilde{\nu}_{\mu 3}$, $\tilde{\nu}_{e1}$, $\tilde{\nu}_{e3}$ roughly gives

$$\begin{aligned}
& (U_{21}^\mu)^2 (U_{21}^e)^2 I(z_{\tilde{\nu}_{\mu 1}}, z_{\tilde{\nu}_{e1}}) - (U_{21}^\mu)^2 (U_{43}^e)^2 I(z_{\tilde{\nu}_{\mu 1}}, z_{\tilde{\nu}_{e3}}) \\
& - (U_{43}^\mu)^2 (U_{21}^e)^2 I(z_{\tilde{\nu}_{\mu 3}}, z_{\tilde{\nu}_{e1}}) + (U_{43}^\mu)^2 (U_{43}^e)^2 I(z_{\tilde{\nu}_{\mu 3}}, z_{\tilde{\nu}_{e3}})
\end{aligned}$$

$$\begin{aligned}
&\approx \frac{m_D^4}{M_R^4} \cdot \frac{\Delta m_{\tilde{\nu}_\mu}^2 \Delta m_{\tilde{\nu}_e}^2}{M_{\tilde{h}_B^-}^4} \frac{\partial}{\partial z_{\tilde{\nu}_{\mu 1}}} \frac{\partial}{\partial z_{\tilde{\nu}_{e 1}}} I(z_{\tilde{\nu}_{\mu 1}}, z_{\tilde{\nu}_{e 1}}) \\
&\sim O\left(\frac{1}{M_R^6}\right),
\end{aligned} \tag{68}$$

while the terms including one light and one heavy sneutrino are roughly

$$\begin{aligned}
&(U_{21}^\mu)^2 (U_{22}^e)^2 I(z_{\tilde{\nu}_{\mu 1}}, z_{\tilde{\nu}_{e 2}}) - (U_{21}^\mu)^2 (U_{44}^e)^2 I(z_{\tilde{\nu}_{\mu 1}}, z_{\tilde{\nu}_{e 4}}) \\
&- (U_{43}^\mu)^2 (U_{22}^e)^2 I(z_{\tilde{\nu}_{\mu 3}}, z_{\tilde{\nu}_{e 2}}) + (U_{43}^\mu)^2 (U_{44}^e)^2 I(z_{\tilde{\nu}_{\mu 3}}, z_{\tilde{\nu}_{e 4}}) \\
&+ (U_{22}^\mu)^2 (U_{21}^e)^2 I(z_{\tilde{\nu}_{\mu 2}}, z_{\tilde{\nu}_{e 1}}) - (U_{22}^\mu)^2 (U_{43}^e)^2 I(z_{\tilde{\nu}_{\mu 2}}, z_{\tilde{\nu}_{e 3}}) \\
&- (U_{44}^\mu)^2 (U_{21}^e)^2 I(z_{\tilde{\nu}_{\mu 4}}, z_{\tilde{\nu}_{e 1}}) + (U_{44}^\mu)^2 (U_{43}^e)^2 I(z_{\tilde{\nu}_{\mu 4}}, z_{\tilde{\nu}_{e 3}}) \\
&\approx \left(\frac{m_D^e}{M_R^e}\right)^2 \cdot \frac{\Delta M_{\tilde{\nu}_\mu}^2 \cdot \Delta m_{\tilde{\nu}_e}^2}{M_{\tilde{h}_B^-}^4} \cdot \left(\frac{M_{\tilde{h}_B^-}}{M_R^\mu}\right)^4 + \left(\frac{m_D^\mu}{M_R^\mu}\right)^2 \cdot \frac{\Delta M_{\tilde{\nu}_e}^2 \cdot \Delta m_{\tilde{\nu}_\mu}^2}{M_{\tilde{h}_B^-}^4} \cdot \left(\frac{M_{\tilde{h}_B^-}}{M_R^e}\right)^4 \\
&\sim O\left(\frac{1}{M_R^6}\right),
\end{aligned} \tag{69}$$

where $\Delta M_{\tilde{\nu}_e}^2$ and $\Delta M_{\tilde{\nu}_\mu}^2$ are the heavy sneutrino squared-mass differences

$$\Delta M_{\tilde{\nu}_e}^2 = 4B_e M_R^e \quad \text{and} \quad \Delta M_{\tilde{\nu}_\mu}^2 = 4B_\mu M_R^\mu. \tag{70}$$

Under our approximations,

$$\Delta M_{\tilde{\nu}_e}^2 = \Delta M_{\tilde{\nu}_\mu}^2 \equiv \Delta M_{\tilde{\nu}}^2 = 4BM_R. \tag{71}$$

The terms including two heavy sneutrinos are roughly

$$\begin{aligned}
&(U_{22}^\mu)^2 (U_{22}^e)^2 I(z_{\tilde{\nu}_{\mu 2}}, z_{\tilde{\nu}_{e 2}}) - (U_{22}^\mu)^2 (U_{44}^e)^2 I(z_{\tilde{\nu}_{\mu 2}}, z_{\tilde{\nu}_{e 4}}) \\
&- (U_{44}^\mu)^2 (U_{22}^e)^2 I(z_{\tilde{\nu}_{\mu 4}}, z_{\tilde{\nu}_{e 2}}) + (U_{44}^\mu)^2 (U_{44}^e)^2 I(z_{\tilde{\nu}_{\mu 4}}, z_{\tilde{\nu}_{e 4}}) \\
&\approx \frac{\Delta M_{\tilde{\nu}_\mu}^2 \cdot \Delta M_{\tilde{\nu}_e}^2}{M_{\tilde{h}_B^-}^4} \cdot \frac{M_{\tilde{h}_B^-}^6}{3M_R^6} \\
&\approx \frac{(\Delta M_{\tilde{\nu}}^2)^2 M_{\tilde{h}_B^-}^2}{3M_R^6} \\
&\sim O\left(\frac{1}{M_R^4}\right).
\end{aligned} \tag{72}$$

Comparing the M_R dependences of Eq.(68), (69) and (72), we see that the dominant term is the one involving two heavy sneutrinos. Thus the contribution from graph (e) and (f) can be approximated as

$$-\frac{(m_D^\mu)^2 (m_D^e)^2}{2048 V_T^4 \pi^2 M_{\tilde{h}_B^-}^2} \cdot \left(\sum_{a=1}^2 \sum_{b=1}^2 (U_{2a}^\mu)^2 (U_{2b}^e)^2 I(z_{\tilde{\nu}_{\mu a}}, z_{\tilde{\nu}_{e b}}) - \sum_{a=1}^2 \sum_{b=3}^4 (U_{2a}^\mu)^2 (U_{4b}^e)^2 I(z_{\tilde{\nu}_{\mu a}}, z_{\tilde{\nu}_{e b}}) \right)$$

$$\begin{aligned}
& - \sum_{a=3}^4 \sum_{b=1}^2 (U_{4a}^\mu)^2 (U_{2b}^e)^2 I(z_{\tilde{\nu}_{\mu a}}, z_{\tilde{\nu}_{eb}}) + \sum_{a=3}^4 \sum_{b=3}^4 (U_{4a}^\mu)^2 (U_{4b}^e)^2 I(z_{\tilde{\nu}_{\mu a}}, z_{\tilde{\nu}_{eb}}) \\
& \approx - \frac{m_D^4 (\Delta M_{\tilde{\nu}}^2)^2}{6144 V_T^4 \pi^2 M_R^6} = - \frac{g_2^4 m_D^4 (\Delta M_{\tilde{\nu}}^2)^2 (1 + \tan^2 \beta)^2}{24576 \pi^2 M_R^6 M_W^4 \tan^4 \beta}.
\end{aligned} \tag{73}$$

Combining the various contributions, the effective coupling constant is thus roughly given by

$$\begin{aligned}
|Re G_{\bar{M}M}| \approx & \left| \frac{g_2^4 m_D^4}{1024 \pi^2 M_R^2 M_W^4} \cdot \ln \frac{M_R}{M_W} - \frac{g_2^4 (\Delta m_{\tilde{\nu}}^2)^2}{2048 \pi^2 M_{\tilde{W}^-}^6} \cdot \frac{\partial}{\partial y_{\tilde{\nu}_{\mu 1}}} \frac{\partial}{\partial y_{\tilde{\nu}_{e 1}}} I(y_{\tilde{\nu}_{\mu 1}}, y_{\tilde{\nu}_{e 1}}) \right. \\
& \left. - \frac{g_2^4 m_D^4 (\Delta M_{\tilde{\nu}}^2)^2 (1 + \tan^2 \beta)^2}{24576 \pi^2 M_R^6 M_W^4 \tan^4 \beta} \right|.
\end{aligned} \tag{74}$$

The first term in Eq.(74) is the dominant contribution of graph (a) and (b), which contains intermediate neutrino and W boson. This contribution appears in the model in which all SUSY partners decoupled. The second term is the dominant contribution of graph (c) and (d), in which wino and sneutrino appear in the intermediate states. Finally, the third term is the dominant contribution of graph (e) and (f), with intermediate higgsino and sneutrinos lines. The second and third terms both depend on the sneutrino mass splitting. This reflects the intra-generation lepton number violating property of the muonium-antimuonium oscillation process, because the sneutrino mass splitting is generated by the $\Delta L = 2$ operators in the sneutrino mass matrix. To compare the relative sizes of these three terms, we use the current experimental limits of the neutrino and sparticle masses.

The first terms in Eq.(74) has a factor m_D^4/M_R^2 , which is the scale of the light neutrino mass square $m_\nu^2 \simeq m_D^4/M_R^2$ generated by see-saw mechanism. The experimental constraints on neutrino masses are summerized in reference[19] as

$$\begin{aligned}
m_\nu(\text{electron based}) & < 225 eV, \\
m_\nu(\text{muon based}) & < 0.19 MeV, \\
m_\nu(\text{tau based}) & < 18.2 MeV,
\end{aligned} \tag{75}$$

For instance, assuming

$$m_D \sim M_W, \tag{76}$$

$$m_\nu = \frac{m_D^2}{M_R} \sim 1 eV, \tag{77}$$

then the right-handed neutrino mass scale is about

$$M_R \sim 10^{13} GeV. \tag{78}$$

In this case, the first terms in Eq.(74) is roughly

$$\frac{g_2^4 m_D^4}{1024\pi^2 M_R^2 M_W^4} \cdot \ln \frac{M_R}{M_W} = \frac{g_2^4 m_\nu^2}{1024\pi^2 M_W^4} \cdot \ln \frac{M_R}{M_W} \simeq 1.1 \times 10^{-29} \text{GeV}^{-2}. \quad (79)$$

The second term in Eq.(74) depends on the light sneutrino squared-mass difference Δm_ν^2 , which can be written in terms of light sneutrino mass splitting $\Delta m_{\tilde{\nu}}$ by

$$\Delta m_\nu^2 = 2m_{\tilde{\nu}}\Delta m_{\tilde{\nu}}, \quad (80)$$

where $m_{\tilde{\nu}}$ is the mass scale of light sneutrinos. So doing the second term in Eq.(74) can be written as

$$-\frac{g_2^4 (\Delta m_\nu^2)^2}{2048\pi^2 M_{\tilde{W}^-}^6} \cdot \frac{\partial}{\partial y_{\tilde{\nu}_{\mu 1}}} \frac{\partial}{\partial y_{\tilde{\nu}_{e 1}}} I(y_{\tilde{\nu}_{\mu 1}}, y_{\tilde{\nu}_{e 1}}) = -\frac{g_2^4 m_\nu^2 (\Delta m_{\tilde{\nu}})^2}{512\pi^2 M_{\tilde{W}^-}^6} \cdot \frac{\partial}{\partial y_{\tilde{\nu}_{\mu 1}}} \frac{\partial}{\partial y_{\tilde{\nu}_{e 1}}} I(y_{\tilde{\nu}_{\mu 1}}, y_{\tilde{\nu}_{e 1}}). \quad (81)$$

Reference [15] provides an upper limit on the sneutrino mass splitting by calculating the one-loop correction to the neutrino mass. Assuming that this correction is no larger than the tree result gives

$$\Delta m_{\tilde{\nu}} \leq 2 \times 10^3 m_\nu. \quad (82)$$

Relaxing this absence of fine tuning constraint can substantially enhance the contribution of the graph (c) and (d). Taking the sneutrino mass splitting to be of the same order as sneutrino mass

$$\Delta m_{\tilde{\nu}} \sim m_{\tilde{\nu}}, \quad (83)$$

and $m_{\tilde{\nu}_\mu}, m_{\tilde{\nu}_e}$ to be the common mass scale $m_{\tilde{\nu}}$ gives

$$y_{\tilde{\nu}_{\mu 1}} \sim y_{\tilde{\nu}_{e 1}} \sim y_{\tilde{\nu}} = \frac{m_{\tilde{\nu}}^2}{M_{\tilde{W}^-}^2}. \quad (84)$$

Eq.(81) can then be written as

$$-\frac{g_2^4 m_\nu^2 (\Delta m_{\tilde{\nu}})^2}{512\pi^2 M_{\tilde{W}^-}^6} \cdot \frac{\partial}{\partial y_{\tilde{\nu}_{\mu 1}}} \frac{\partial}{\partial y_{\tilde{\nu}_{e 1}}} I(y_{\tilde{\nu}_{\mu 1}}, y_{\tilde{\nu}_{e 1}}) \approx -\frac{g_2^4 m_\nu^4}{512\pi^2 M_{\tilde{W}^-}^6} \cdot \frac{\partial}{\partial y_{\tilde{\nu}_{\mu 1}}} \frac{\partial}{\partial y_{\tilde{\nu}_{e 1}}} I(y_{\tilde{\nu}_{\mu 1}}, y_{\tilde{\nu}_{e 1}}) \Big|_{y_{\tilde{\nu}_{\mu 1}}, y_{\tilde{\nu}_{e 1}} = y_{\tilde{\nu}}}. \quad (85)$$

The function $\frac{m_\nu^4}{M_{\tilde{W}^-}^6} \cdot \frac{\partial}{\partial y_{\tilde{\nu}_{\mu 1}}} \frac{\partial}{\partial y_{\tilde{\nu}_{e 1}}} I(y_{\tilde{\nu}_{\mu 1}}, y_{\tilde{\nu}_{e 1}}) \Big|_{y_{\tilde{\nu}_{\mu 1}}, y_{\tilde{\nu}_{e 1}} = y_{\tilde{\nu}}}$ in Eq.(85) is a decreasing function of $M_{\tilde{W}^-}$. In order to calculate the maximum contribution of graph (c) and (d), we use the experimental lower bound on $M_{\tilde{W}^-}$. Many experimental searches for physics beyond the standard model have been conducted and provide various constraints on SUSY parameter space. Tab.3 lists some of the constraints[18].

Sparticle	lower limit [GeV]	Sparticle	lower limit [GeV]
$\tilde{\chi}_1^\pm$	94.0	$\tilde{\mu}_R$	94.0
$\tilde{\chi}_1^0$	46.0	\tilde{e}_L	107.0
$\tilde{\nu}$	94.0	\tilde{e}_R	73.0

Table 3: Experimental lower limits on SUSY particle masses

Fixing the wino mass to its lower limit in Tab.3

$$M_{\tilde{W}^-} = 94.0 GeV, \quad (86)$$

the contribution $\frac{g_2^4 m_{\tilde{\nu}}^4}{512\pi^2 M_{\tilde{W}^-}^6} \cdot \frac{\partial}{\partial y_{\tilde{\nu}\mu 1}} \frac{\partial}{\partial y_{\tilde{\nu}e 1}} I(y_{\tilde{\nu}\mu 1}, y_{\tilde{\nu}e 1}) \Big|_{y_{\tilde{\nu}\mu 1}, y_{\tilde{\nu}e 1} = y_{\tilde{\nu}}}$ as a function of sneutrino mass scale $m_{\tilde{\nu}}$ is shown in Fig.2.

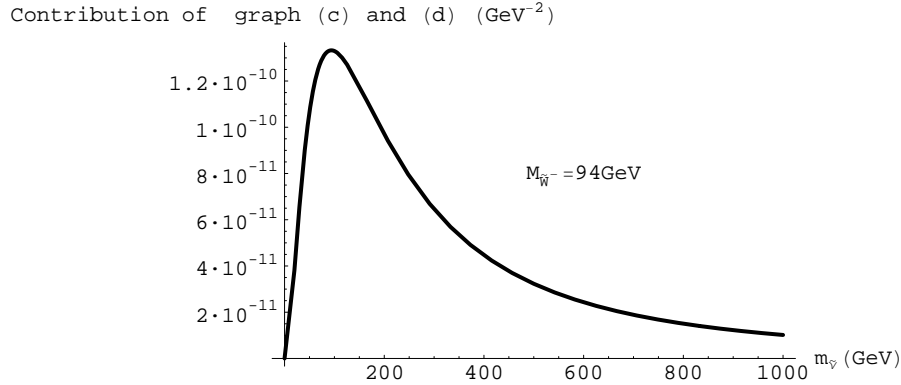


Figure 2: The contribution of graph (c) and (d) as a function of $m_{\tilde{\nu}}$ when fixing the wino mass to its lower limit $M_{\tilde{W}^-}$.

When $m_{\tilde{\nu}} = 94.0 GeV$, which is allowed by the experimental limit in Tab.3, the contribution of graph (c) and (d) reaches its maximum so that

$$\frac{g_2^4 m_{\tilde{\nu}}^4}{512\pi^2 M_{\tilde{W}^-}^6} \cdot \frac{\partial}{\partial y_{\tilde{\nu}\mu 1}} \frac{\partial}{\partial y_{\tilde{\nu}e 1}} I(y_{\tilde{\nu}\mu 1}, y_{\tilde{\nu}e 1}) \Big|_{y_{\tilde{\nu}\mu 1}, y_{\tilde{\nu}e 1} = y_{\tilde{\nu}}} \leq 1.3 \times 10^{-10} GeV^{-2}. \quad (87)$$

Finally, the third term in Eq.(74) depends on the heavy sneutrino squared-mass difference $\Delta M_{\tilde{\nu}}^2 = 2M_{\tilde{\nu}}\Delta M_{\tilde{\nu}} = 4BM_R$. Since we assume that M_R is the largest mass scale, $\Delta M_{\tilde{\nu}}$ can't be arbitrarily large. Taking parameter B one order of magnitude smaller than M_R , the heavy sneutrino mass splitting is

$$\Delta M_{\tilde{\nu}} \sim \frac{M_R}{10}. \quad (88)$$

The contribution of graph (e) and (f) can then be written as

$$\frac{g_2^4 m_D^4 (\Delta M_{\tilde{\nu}}^2)^2 (1 + \tan^2 \beta)^2}{24576 \pi^2 M_R^6 M_W^4 \tan^4 \beta} = \frac{g_2^4 m_{\nu}^2 (1 + \tan^2 \beta)^2}{614400 \pi^2 M_W^4 \tan^4 \beta}. \quad (89)$$

When $\tan \beta$ is very small the contribution can get large and even reach the experimental limit Eq.(59). In this case, the experimental limit of muonium-antimuonium oscillation provides an inequality relating $\tan \beta$ and m_{ν} , which is given by

$$\frac{g_2^4 m_{\nu}^2 (1 + \tan^2 \beta)^2}{614400 \pi^2 M_W^4 \tan^4 \beta} \leq 3.5 \times 10^{-8} \text{GeV}^{-2}. \quad (90)$$

This inequality translates into a lower bound of $\tan \beta$ for different light neutrino masses m_{ν} :

$$\begin{aligned} \tan \beta &\geq 3.7 \times 10^{-7}, & \text{if } m_{\nu} &= 1 \text{eV}, \\ \tan \beta &\geq 3.7 \times 10^{-8}, & \text{if } m_{\nu} &= 10^{-2} \text{eV}, \\ \tan \beta &\geq 3.7 \times 10^{-9}, & \text{if } m_{\nu} &= 10^{-4} \text{eV}. \end{aligned} \quad (91)$$

The lower limit on $\tan \beta$ as a function of light neutrino mass scale m_{ν} is shown in Fig.3.

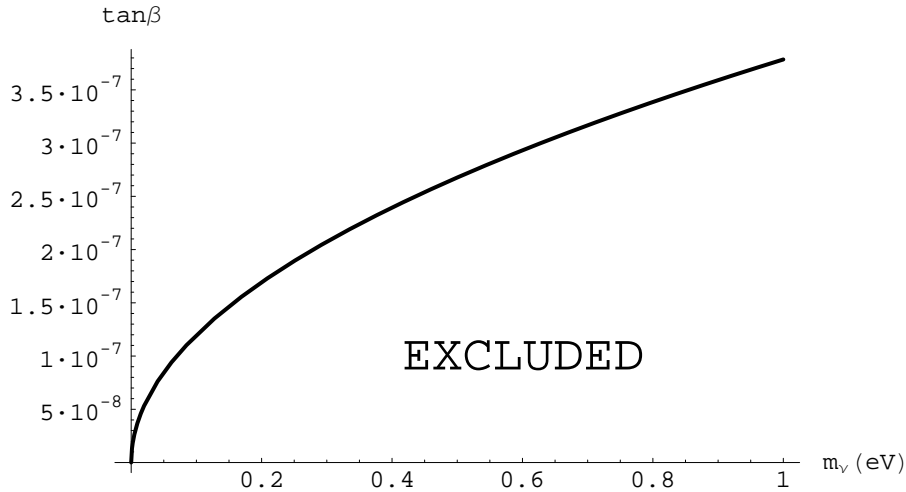


Figure 3: The lower limit on $\tan\beta$ as a function of light neutrino mass scale m_ν provided by the muonium-antimuonium oscillation experiment. The area above the curve is allowed by the experiment results.

Notice that the ratio of the two Higgs VEVs $\tan\beta$ are related to the light neutrino masses in the above inequality, although the graph (e) and (f) don't involve any neutrinos in the intermediate states. This results since we are using a specific model where the neutrino masses are generated by see-saw mechanism $m_\nu \sim O(m_D^2/M_R)$. The sneutrino mixing matrix is approximated in term of m_D/M_R and the heavy sneutrino masses are also of order M_R . If we take m_D to be of order M_W , the heavy sneutrino masses M_R in the contribution of graph (e) and (f) can be expressed in term of the light neutrino mass scale m_ν . This explains the appearance of the parameter m_ν in the inequality Eq.(90).

However, for non-infinitesimal values of $\tan\beta$, this contribution is very small compared with the maximum of the second term in Eq.(74). For instance, taking the neutrino mass m_ν to be $1eV$ and assuming $\tan\beta \geq 10^{-4}$, the contribution of graph (e) and (f) is

$$\frac{g_2^4 m_\nu^2 (1 + \tan^2 \beta)^2}{614400 \pi^2 M_W^4 \tan^4 \beta} \lesssim 7.2 \times 10^{-18} GeV^{-2}. \quad (92)$$

Thus, except for the case of very small $\tan\beta$, the second term in Eq.(74) is the dominant contribution for a wide range of the parameters and its maximum is roughly two orders of magnitude below the sensitivity of the current experiments.

6 The constraints from the muon and electron anomalous magnetic moment experiments

One has to be careful about other constraints on the model parameters. Examples of such potential constraints come from the measurements of the muon and electron anomalous magnetic moments. The correction to the muon anomalous magnetic moment in the model under consideration is found by calculating the one-loop graphs shown in Fig.4.

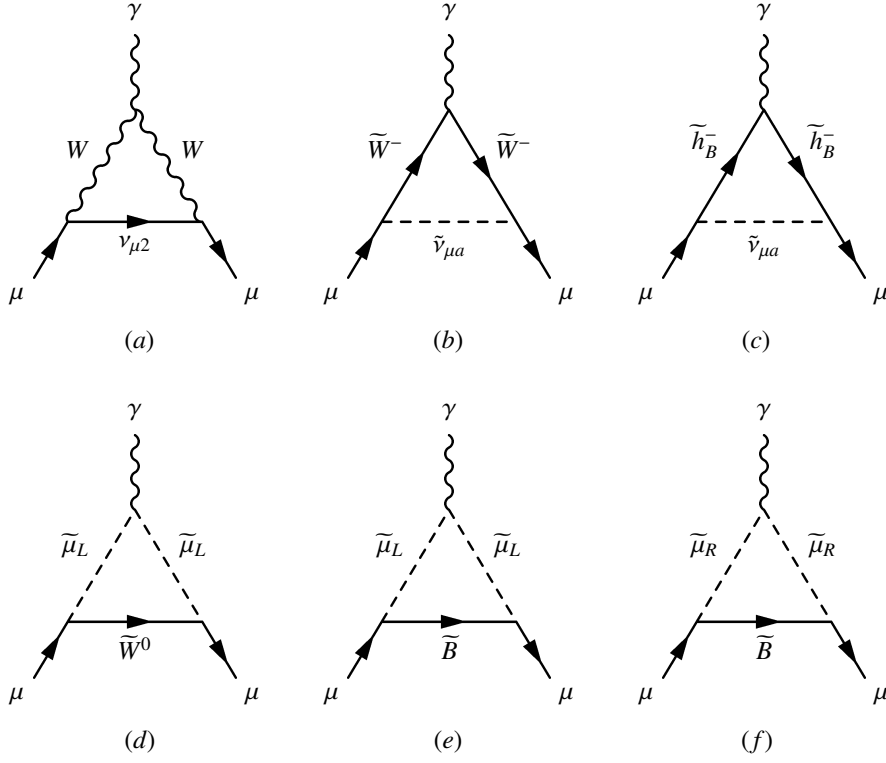


Figure 4: The Feynman graphs contributing to the muon anomalous magnetic moment beyond the Standard Model.

The muon anomalous magnetic moment contributed from the above graphs is

$$\begin{aligned}
a_{\mu}^{BSM} = & -\frac{g_2^2 m_{\mu}^2}{16\pi^2 M_W^2} (V_{12}^{\mu} V_{12}^{\mu*})^2 F^W(x_{\nu_{\mu 2}}) \\
& + \frac{g_2^2 m_{\mu}^2}{32\pi^2 M_{\tilde{W}^-}^2} \left(\sum_{a=1}^2 (U_{1a}^{\mu})^2 F^C(y_{\tilde{\nu}_{\mu a}}) + \sum_{a=3}^4 (U_{3a}^{\mu})^2 F^C(y_{\tilde{\nu}_{\mu a}}) \right) \\
& + \frac{(m_D^{\mu})^2 m_{\mu}^2}{32\pi^2 V_T M_{\tilde{h}_B^-}^2} \left(\sum_{a=1}^2 (U_{2a}^{\mu})^2 F^C(z_{\tilde{\nu}_{\mu a}}) + \sum_{a=3}^4 (U_{4a}^{\mu})^2 F^C(z_{\tilde{\nu}_{\mu a}}) \right) \\
& - \frac{g_2^2 m_{\mu}^2}{32\pi^2 M_{\tilde{W}^0}^2} F^N(s_{\tilde{\mu}_L}) - \frac{g_2^2 m_{\mu}^2}{32\pi^2 M_{\tilde{B}}^2} F^N(t_{\tilde{\mu}_L}) - \frac{g_1^2 m_{\mu}^2}{8\pi^2 M_{\tilde{B}}^2} F^N(t_{\tilde{\mu}_R}), \quad (93)
\end{aligned}$$

where $s_{\tilde{\mu}_a} = \frac{m_{\tilde{\mu}_a}^2}{M_{\tilde{W}^0}^2}$, $t_{\tilde{\mu}_a} = \frac{m_{\tilde{\mu}_a}^2}{M_{\tilde{B}}^2}$, and

$$F^W(x_{\nu_{\mu 2}}) = \int_0^1 dx \frac{-4x^2(1+x) - 2x_{\mu} \cdot x^2(x-1) - 2x_{\nu_{\mu 2}}(2x - 3x^2 + x^3)}{x_{\mu} \cdot x^2 + (1-x_{\mu})x + x_{\nu_{\mu 2}}(1-x)}, \quad (94)$$

$$F^C(y_{\tilde{\nu}_{\mu a}}) = \frac{2y_{\tilde{\nu}_{\mu a}}^3 - 3y_{\tilde{\nu}_{\mu a}}^2(-1 + 2 \ln y_{\tilde{\nu}_{\mu a}}) - 6y_{\tilde{\nu}_{\mu a}} + 1}{6(1 - y_{\tilde{\nu}_{\mu a}})^4}, \quad (95)$$

$$F^N(s_{\tilde{\mu}_a}) = \frac{s_{\tilde{\mu}_a}^3 - 6s_{\tilde{\mu}_a}^2 + 3s_{\tilde{\mu}_a} + 6s_{\tilde{\mu}_a} \ln s_{\tilde{\mu}_a} + 2}{6(1 - s_{\tilde{\mu}_a})^4}. \quad (96)$$

With assumption that M_R is the largest mass scale, the dominant contribution of the graphs in Fig.4 to a_{μ}^{BSM} is

$$\begin{aligned} a_{\mu}^{BSM} \approx & \frac{g_2^2 m_{\mu}^2 m_D^2}{12\pi^2 M_{\tilde{W}}^2 M_R^2} + \frac{g_2^2 m_{\mu}^2}{32\pi^2 M_{\tilde{W}^-}^2} \cdot (F^C(y_{\tilde{\nu}_{\mu 1}}) + F^C(y_{\tilde{\nu}_{\mu 3}})) + \frac{g_2^2 m_{\mu}^2 m_D^2 (1 + \tan^2 \beta)}{96\pi^2 M_{\tilde{W}}^2 M_R^2 \tan^2 \beta} \\ & - \frac{g_2^2 m_{\mu}^2}{32\pi^2 M_{\tilde{W}^0}^2} F^N(s_{\tilde{\mu}_L}) - \frac{g_2^2 m_{\mu}^2}{32\pi^2 M_{\tilde{B}}^2} F^N(t_{\tilde{\mu}_L}) - \frac{g_1^2 m_{\mu}^2}{8\pi^2 M_{\tilde{B}}^2} F^N(t_{\tilde{\mu}_R}). \end{aligned} \quad (97)$$

The second and the last three terms are all decreasing functions of slepton, chargino and neutralino masses. We can use the experimental bounds in Tab.3 to calculate the maximum values of these terms yielding

$$\begin{aligned} \frac{g_2^2 m_{\mu}^2}{32\pi^2 M_{\tilde{W}^-}^2} \cdot (F^C(y_{\tilde{\nu}_{\mu 1}}) + F^C(y_{\tilde{\nu}_{\mu 3}})) & \leq 2.5 \times 10^{-10}, \\ \frac{g_2^2 m_{\mu}^2}{32\pi^2 M_{\tilde{W}^0}^2} F^N(s_{\tilde{\mu}_L}) & \leq 1.9 \times 10^{-10}, \\ \frac{g_2^2 m_{\mu}^2}{32\pi^2 M_{\tilde{B}}^2} F^N(t_{\tilde{\mu}_L}) & \leq 1.9 \times 10^{-10}, \\ \frac{g_1^2 m_{\mu}^2}{8\pi^2 M_{\tilde{B}}^2} F^N(t_{\tilde{\mu}_R}) & \leq 2.1 \times 10^{-10}. \end{aligned} \quad (98)$$

The maxima of these terms are all about one order of magnitude smaller than the present experimental bound on the contribution to $a_{\mu} = \frac{1}{2}(g-2)$ beyond the standard model [16]:

$$\delta a_{\mu} = a_{\mu}^{exp} - a_{\mu}^{SM} = 2 \times 10^{-9}. \quad (99)$$

The first and third term both depend on the light neutrino mass scale m_{ν} and get suppressed. For instance, using the assumptions Eq.(76) and Eq.(77), the first and third terms are

$$\frac{g_2^2 m_{\mu}^2 m_D^2}{12\pi^2 M_{\tilde{W}}^2 M_R^2} = \frac{g_2^2 m_{\mu}^2 m_{\nu}^2}{12\pi^2 M_{\tilde{W}}^4} \approx 8.7 \times 10^{-31},$$

$$\frac{g_2^2 m_\mu^2 m_D^2 (1 + \tan^2 \beta)}{96\pi^2 M_W^2 M_R^2 \tan^2 \beta} = \frac{g_2^2 m_\mu^2 m_\nu^2 (1 + \tan^2 \beta)}{96\pi^2 M_W^4 \tan^2 \beta} \approx 1.1 \times 10^{-31} \cdot \frac{1 + \tan^2 \beta}{\tan^2 \beta}. \quad (100)$$

The first term is negligible compared with the terms in Eq.(99). However, the third term can be large if $\tan\beta$ is very small. Therefore, the experimental bound on the muon magnetic moment will provide an inequality on $\tan\beta$ and m_ν , which is given by

$$\frac{g_2^2 m_\mu^2 m_\nu^2 (1 + \tan^2 \beta)}{96\pi^2 M_W^4 \tan^2 \beta} \leq 2 \times 10^{-9}. \quad (101)$$

This inequality translates into a lower bound on $\tan\beta$ as a function of the light neutrino mass scale m_ν as shown in Fig.5.

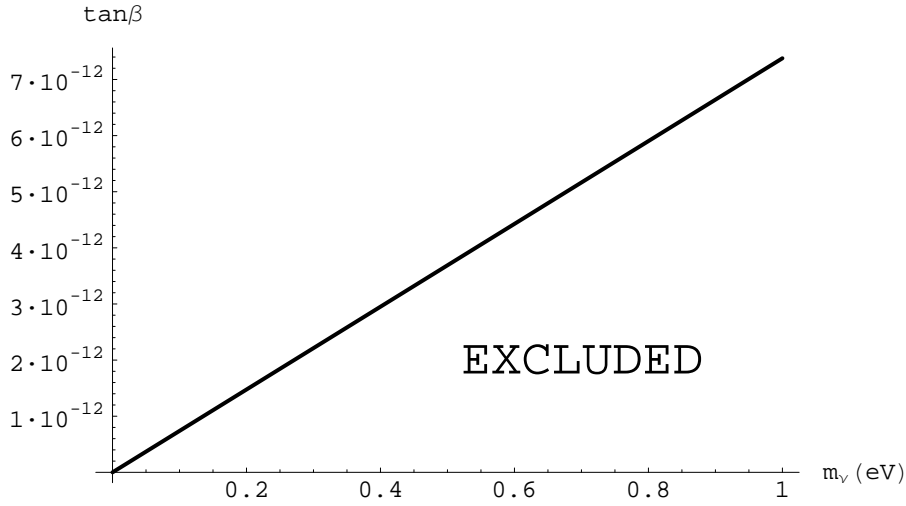


Figure 5: The lower limit on $\tan\beta$ as a function of light neutrino mass scale m_ν provided by the muon anomalous magnetic moment experiment. The area above the curve is allowed by the experiment results.

The electron anomalous magnetic moment beyond the Standard Model is contributed by the six Feynman graphs displayed in Fig.6.

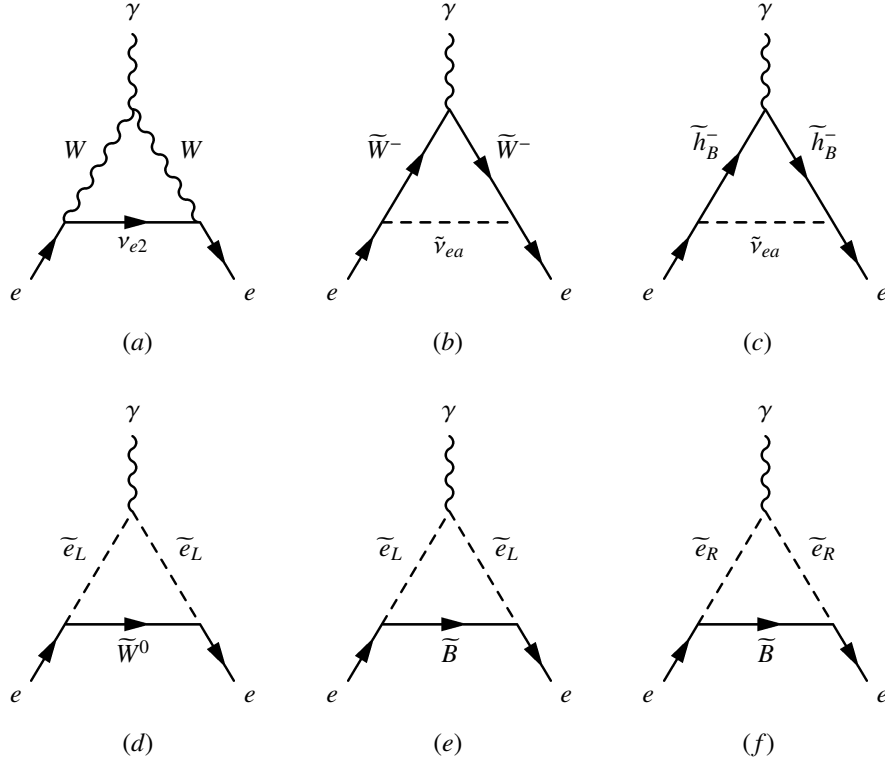


Figure 6: The Feynman graphs contributing to the electron anomalous magnetic moment beyond the Standard Model.

The experimental bound on the contribution to the electron anomalous magnetic moment beyond Standard Model is[17]

$$\delta a_e = a_e^{exp} - a_e^{SM} = 1.4 \times 10^{-11}. \quad (102)$$

In analogy to the muon case, this experimental limit will also generate an inequality relation of m_ν and $\tan\beta$ given by

$$\frac{g_z^2 m_e^2 m_\nu^2 (1 + \tan^2 \beta)}{96 \pi^2 M_W^4 \tan^2 \beta} \leq 1.4 \times 10^{-11}. \quad (103)$$

This inequality is illustrated in Fig.7.

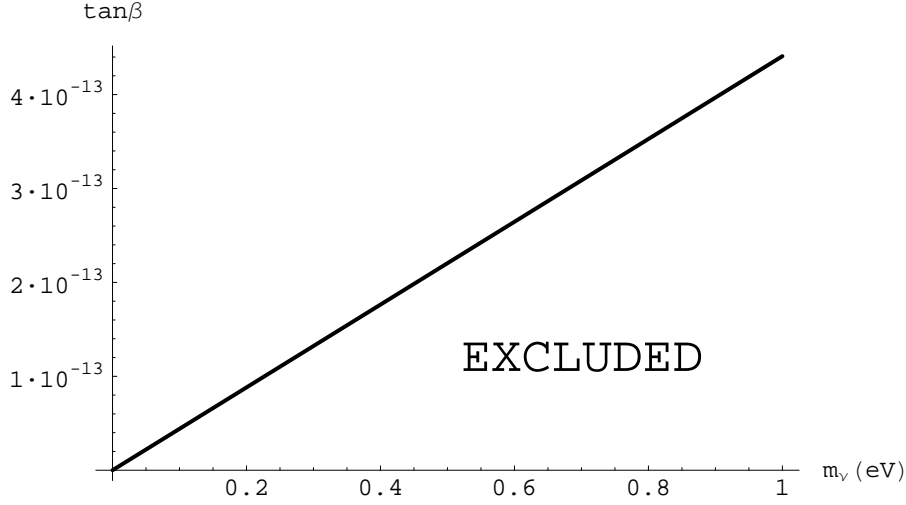


Figure 7: The lower limit on $\tan\beta$ as a function of light neutrino mass scale m_ν provided by the electron anomalous magnetic moment experiment. The area above the curve is allowed by the experiment results.

From Fig.2, Fig.5 and Fig.7 we see that for the model we are considering, the muonium-antimuonium oscillation experiment gives a more stringent constraint on $\tan\beta$ than the muon and electron anomalous magnetic moment experiments.

7 Conclusions

We have calculated the effective coupling constant of the muonium-antimuonium oscillation process in the Minimal Supersymmetric Standard Model extended by inclusion of three right-handed neutrino superfields where the required lepton flavor violation has its origin in the Majorana property of the neutrino and sneutrino mass eigenstates. For a wide range of the parameters, the contribution of the graphs mediated by the sneutrino and winos \widetilde{W}^- is dominant. The maximum of this contribution to the effective coupling constant is roughly two orders of magnitude below the sensitivity of current muonium-antimuonium oscillation experiments. However, there is very limited possibility that the contribution of the graphs mediated by sneutrinos and Higgsino \widetilde{h}_B^- is dominant if $\tan\beta$ is very small. In this case, the contributions can even be large enough to reach the present experimental bound. Therefore, the experimental bound can provide an inequality on

the model parameters, which can be translated into a lower bound on $\tan\beta$ as a function of light neutrino mass scale m_ν . The constraints from the muon and electron anomalous magnetic moments were also investigated. For this model, the muonium-antimuonium oscillation experiments give the most stringent constraints on the parameters.

Acknowledgements

It's a pleasure to thank Professor S. T. Love, Professor T. E. Clark and Chi Xiong for useful discussions.

References

- [1] For a general review of present state of oscillation phenomena in neutral meson systems, see, for example, M. Battaglia et al., The CKM Matrix and the Unitarity Triangle, in the *Workshop on CKM Unitarity Triangle* (CERN 2002-2003), Geneva, Switzerland, 13-16 Feb 2002, hep-ph/0304132.
- [2] For a general discussion of mixing in the neutral $K^0 - \bar{K}^0$ and $B^0 - \bar{B}^0$, see, for example, A. Buras, in *International School of Subnuclear Physics: 38th Course: Theory and Experiment Heading for New Physics*, Erice, 2000, hep-ph/0101336.
- [3] Analogous oscillation phenomena has also been speculated upon for the neutron-antineutron system. Here the mixing matrix elements arise from an underlying baryon number violating grand unified theory. For various discussions, see, S. Glashow, in *Proceedings of Neutrino 79, International Conference on Neutrinos, Weak Interactions and Cosmology*, Bergen, Norway, 1979, ed. by A. Haatuft and C. Jarlskog (Fysik Institutt, Bergen, 1980); R.E. Marshak and R. N. Mohapatra, Phys. Rev. Lett. **44**, 1316 (1980); T.K. Kuo and S.T. Love, Phys. Rev. Lett. **45**, 93 (1980).
- [4] B.Pontecorvo, Sov.Phys.JETP **6**, 429 (1957).
- [5] T. Huber et al., Phys. Rev. D **41**, 2709 (1990); B. Matthias et al., Phys. Rev. Lett. **66**, 2716 (1991); R. Abela et al., Phys. Rev. Lett. **77**, 1950 (1996).
- [6] L. Willmann et al, Phys. Rev. Lett **82**, 49 (1999).
- [7] A. Halprin, Phys. Rev. Lett **48**, 1313 (1982).

- [8] P.Herczeg and R. N. Mohapatra, Phys. Rev. Lett. **69**, 2475 (1992).
- [9] T. E. Clark and S. T. Love, Mod. Phys. Lett. **A19**, 297 (2004).
- [10] G.Cvetic, C.O.Dib, C.S.Kim and J.D.Kim, Phys.Rev.D **71**, 113013 (2005).
- [11] Boyang Liu, “Gauge Invariance of the Muonium-Antimuonium Oscillation Time Scale and Limits on Right-Handed Neutrino Masses”, arXiv:0806.0884.
- [12] A.Halprin and A.Masiero, Phys. Rev. D **48**, R2987 (1993).
- [13] Stephen P. Martin, “A supersymmetry Primer”, hep-ph/9709356.
- [14] P. Minkowski, Phys. Lett. **B67**, 421 (1977); T. Yanagida, in *Proceedings of the Workshop on the Unified Theories and Baryon Number in the Universe*, Tsukuba, Japan, 1979, (O. Sawada and A. Sugamoto eds), p95; M. Gell-Mann, P. Ramond and R. Slansky in *Supergravity*, (P. van Nieuwenhuizen and D. Freedman eds) North-Holland, Amsterdam, 1979; S.L. Glashow, in *Proceedings of the 1979 Cargese Institute on Quarks and Leptons* (M. Levy et. al. eds.) Plenum Press, New York 1980, p687; R.N. Mohapatra and G. Senjanovic. Phys. Rev. Lett. **44**, 912 (1980).
- [15] Yuval Grossman and Howard E.Haber, Phys.Rev. Lett. **78**, 3438 (1997).
- [16] Kirill Melnikov and Arkady Vainshtein, *Theory of the Muon Anomalous Magnetic Moment*, (Springer), 2006, p. 152.
- [17] John R. Ellis, Marek Karliner, Mark A. Samuel and Eric Steinfelds, SLAC-PUB-6670, CERN-TH-7451-94, TAUP-2001-94, OSU-RN-293, hep-ph/9409376.
- [18] J.-F.Grivaz, Phys. Lett. **B667**, 1228 (2008).
- [19] P. Vogel and A. Piepke, Phys. Lett. **B667**, 517 (2008).